Modeling and CW Operation of a Quasi-Three-Level 946 nm Nd:YAG Laser

TSO YEE FAN, STUDENT MEMBER, IEEE, AND ROBERT L. BYER, SENIOR MEMBER, IEEE

Abstract—A model is developed for an end-pumped quasi-three-level laser with population in the lower laser level at equilibrium such as for transitions to the manifolds $^4I_{9/2}$ in Nd^{3+}, $^4I_{15/2}$ in Er^{3+}, $^5I_8$ in Ho^{3+} and $^3H_6$ in Tm^{3+}. It is shown that the effect of residual lower laser level population on laser operation can be treated as a saturable loss. Room temperature operation on the $^4F_{3/2}$–$^4I_{9/2}$ transition in Nd:YAG under CW dye laser pumping has been demonstrated with a threshold as low as 11.5 mW incident power and a slope efficiency of 7 percent with 0.3 percent output coupling. Performance is limited by the low output coupling and diffraction loss.

I. INTRODUCTION

Nd^{3+}-DOPED solid-state lasers have been demonstrated on four transitions from the $^4F_{3/2}$ manifold in the wavelength regions 0.93, 1.05, 1.32, and 1.8 μm corresponding to lower manifolds of $^4I_{9/2}$, $^4I_{11/2}$, $^4I_{13/2}$, and $^4I_{15/2}$, respectively. The vast majority of these lasers operate on either the $^4F_{3/2}$–$^4I_{11/2}$ or $^4F_{3/2}$–$^4I_{13/2}$ transitions. One difficulty with the $^4F_{3/2}$–$^4I_{9/2}$ transition is a lower gain leading to parasitic oscillation on the higher gain transitions, $^4F_{3/2}$–$^4I_{11/2}$, especially when operating in a pulsed mode. Another difficulty is that the lower laser level is in the ground-state manifold. The degeneracy of the ground-state manifold energy levels is lifted by the crystal field splitting, but the total splitting is typically only 800 cm^{-1} for garnet materials and less in other crystals. For a lower laser level at 800 cm^{-1}, there is still significant lower laser level population at room temperature which increases the threshold. To suppress parasitic oscillation, dichroic coatings [1] and intracavity prisms [2], [3], have been used. In addition, the crystal has been cooled to reduce the lower state population [1], [2] and thereby reduce the threshold for the $^4F_{3/2}$–$^4I_{9/2}$ transition.

Three continuous wave (CW) room temperature lasers on this transition have been demonstrated. One is Nd:CAMGAR [4] which was end-pumped by an Ar^+ laser operating at 514.5 nm with a threshold of approximately 400 mW absorbed power with 1 percent transmitting output mirror under quasi-CW excitation. However, using the same apparatus, laser action on this transition in Nd:YAG could not be achieved because of the high gain at 1.06 μm. CW operation was recently demonstrated in a Nd:glass single-mode fiber laser pumped by a rhodamine 6G dye laser with a threshold of ~8 mW [5]. This low threshold was obtained by confining the pump and laser modes to small cross-sectional areas. More recently, diode laser pumped operation of a fiber laser was achieved with a 4.3 mW absorbed power threshold [6].

There has been much recent interest in using semiconductor diode lasers as pump sources for Nd-doped lasers [7], [8]. It is interesting to see whether diode laser pumping is possible at or near room temperature on the $^4I_{9/2}$ transition in a nonguided wave device. This transition may be particularly interesting for diode pumping because of the small quantum defect (i.e., small difference between the pump photon and laser photon energies) which may ultimately allow higher overall efficiencies and the potential to intracavity double this wavelength to the blue as has been recently demonstrated in the green [9]–[12].

In this paper, we model CW laser threshold and output on transitions with significant lower laser level populations. These include the 946 nm Nd:YAG transition as well as many other transitions in other rare-earth ion doped materials such as the $^5I_7$–$^5I_8$ transition in Ho^{3+}, the $^3F_4$–$^3H_6$ transition in Tm^{3+}, and the $^4I_{13/2}$–$^4I_{15/2}$ transition in Er^{3+}. In some cases, even the $^4F_{3/2}$–$^4I_{11/2}$ transition in Nd^{3+} is in this category although it is typically considered to be a four-level system [13]–[15]. We also demonstrate experimentally that the laser threshold for the $^4F_{3/2}$–$^4I_{9/2}$ transition in Nd:YAG at 946 nm is low enough to permit diode laser pumping.

II. THEORY

A. The Quasi-Three-Level Laser Model

The goal of this paper is to model laser operation for end-pumped lasers with significant lower laser level population. We refer to this system as a quasi-three-level laser. There are a number of calculations of a similar type which have been made for four-level lasers [16]–[23] which can be used to develop this model. The approach taken in this paper involves using the overlap between the laser cavity mode and the pump mode and parallels that of Kubodera and Otsuka [18] and Kubodera *et al.* [19]. These earlier works assumed four-level laser operation with an unpopulated lower laser level; in this work we account for population in the lower laser level at equilibrium.

Manuscript received November 3, 1986; revised December 15, 1986. This work was supported by the U.S. Office of Naval Research.
The authors are with the Edward L. Ginzton Laboratory, Stanford University, Stanford, CA 94305.
IEEE Log Number 8613305.

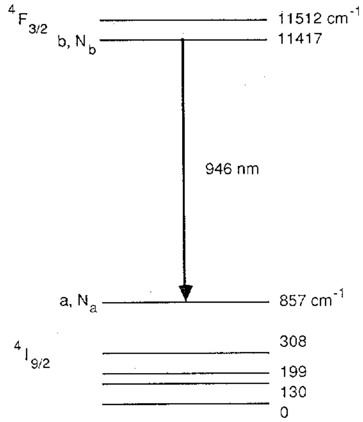

Fig. 1. Energy level diagram of the 946 nm Nd : YAG laser. The levels of the upper and lower manifolds and their energies are shown. The laser transition is noted by the heavy line. The populations of the upper and lower laser level, b and a, are given by N_b and N_a, respectively.

The active ion has an energy level diagram as shown in Fig. 1 with the laser transition as noted. The relative populations of the levels in the lower manifold are given by a Boltzmann distribution. The lower laser level population is then

$$N_a = \frac{g_a N_0}{Z_a} \exp\left(-E_a/kT\right) = f_a N_0 \tag{1a}$$

where

$$Z_a = \sum_i g_i \exp\left(-\frac{\mathrm{E}_i}{\mathrm{kT}}\right) \tag{1b}$$

is the partition function, N_a is the lower laser level population, E_a is its energy, k is the Boltzmann constant, T is the temperature, f_a is the fractional population in the level, g_i and g_a are the degeneracies of states i and a, and N_0 is the total dopant concentration. The sum is over all states in the lower manifold. In steady-state pumping, the relative populations of the levels in the upper manifold can also be described by a Boltzmann distribution if the relaxation between the levels in the upper manifold is rapid. The upper laser level population, N_b, is given by $f_b N_1$ as in (1) where N_1 is the total upper manifold population.

The following models developed in this paper for both threshold and output assume that the population of the upper manifold is always small compared to the total doping level, $N_1 << N_0$; that is, the population of the ground manifold is not significantly reduced. This approximation of no depletion of the ground-state population is good only for some laser transitions to the ground state manifold. The validity of this approximation can be defined in terms of spectroscopic properties of the laser transition and ion, in particular f_a and f_b. If it is assumed that there are no cavity losses, then the threshold condition is $f_b N_1 = f_a N_0$. Now, for no depletion of the ground state the condition $N_1 << N_0$ applies. So, combining this last condition with the threshold condition, at threshold the approximation of no ground-state depletion is equivalent to $f_a/f_b << 1$. This last condition defines the laser transitions for which the following models are valid.

This treatment considers only the fundamental TEM_{00} laser cavity mode with a Gaussian intensity distribution. The effects of diffraction in the gain medium are ignored. The pump beam is also Gaussian with no diffraction and is assumed to pass only once through the gain medium. The geometry is an end-pumped laser with a solid-state laser medium of length L. In this case, normalized pump and cavity modes, $r_p(r, z)$ and $s_0(r, z)$ respectively, in the crystal are given by

$$r_p(r, z) = \frac{2\alpha}{\pi w_p^2[1 - \exp(-\alpha L)]} \exp(-\alpha z) \cdot \exp\left(-\frac{2r^2}{w_p^2}\right) \tag{2a}$$

$$s_0(r, z) = \frac{2}{\pi w_0^2 L} \exp\left(-\frac{2r^2}{w_0^2}\right) \tag{2b}$$

where

$$\iiint s_0(r, z)\, dV = \iiint r_p(r, z)\, dV = 1. \tag{2c}$$

These modes are represented in tems of normalized intensity as opposed to electric field amplitude. α is the intensity absorption coefficient at the pump wavelength and w_p and w_0 are the Gaussian beam radii for the pump and laser cavity modes defined such that the electric field amplitude at $r = w_p$, w_0 is $1/e$ of that at $r = 0$.

B. Threshold Calculation

In this model we use the rate equation approach to derive the populations of the upper laser level and lower laser level and the threshold condition that the round-trip gain exceeds the round-trip loss. The upper laser level population in steady-state at or below threshold is given by the rate equation

$$\frac{dN_1(r, z)}{dt} = 0 = -\frac{N_1(r, z)}{\tau} + R r_p(r, z). \tag{3}$$

It follows that

$$N_b(r, z) = f_b N_1(r, z) = f_b R r_p(r, z) \tau \tag{4}$$

where R is the total pump rate and τ is the lifetime of the upper laser manifold. This equation ignores depletion of the lower manifold population. Since the lower laser level has a small population compared to the total dopant concentration, the upper-state population required to reach threshold is also small so the approximation is valid.

The condition for threshold is that there be enough upper laser level population that the round-trip gain averaged over the cavity mode equals the round-trip loss. In the low loss approximation, this condition is

$$\iiint 2\sigma_a L s_0(r, z) \left[f_b N_1(r, z)\, g_a/g_b - f_a N_0\right] dV = \delta \tag{5}$$

where σ_a is the absorption cross section, and δ is the round-trip cavity loss. The stimulated emission cross section, σ_b, is related to the absorption cross section by $\sigma_b = \sigma_a g_a / g_b$. In Nd:YAG, each level has a degeneracy of 2, so the degeneracy factor cancels. For the purpose of this model we set $\sigma_a = \sigma_b = \sigma$. Substituting (4) into (5) and performing the integration, the condition for threshold becomes

$$R_{\text{th}} \iiint s_0(r, z)\, r_p(r, z)\, dV = \frac{1}{f_b \tau} \left(\frac{\delta}{2\sigma L} + f_a N_0 \right) \quad (6)$$

where R_{th} is the threshold pump rate. R_{th} is related to the absorbed threshold pump power by $P'_{\text{th}} = R_{\text{th}} h\nu_p / \eta_p$ where $h\nu_p$ is the pump photon energy, and η_p is the pump quantum efficiency, the number of ions in the upper last level created by each absorbed photon. Performing the integration, solving for R_{th} in (6), and using the relation between P'_{th} and R_{th}, one obtains

$$P'_{\text{th}} = \frac{\pi h\nu_p}{2 f_p \eta_p \tau} (w_0^2 + w_p^2) \left(\frac{\delta}{2\sigma} + f_a N_0 L \right) \quad (7a)$$

$$P_{\text{th}} = P'_{\text{th}} / [1 - \exp(-\alpha L)] \quad (7b)$$

where P'_{th} is the absorbed power, and P_{th} is the incident pump power at threshold. Equation (7) is the same as that for a four-level laser [19] except for the additional term $f_a N_0 L$ which is due to the need to overcome lower laser level population.

P_{th} and P'_{th} can be differentiated with respect to L to find the crystal length which give the lowest threshold. When P'_{th} is differentiated a positive constant is obtained which means that the minimum absorbed pump power for threshold is for $L = 0$ because the number of lower laser ions in the cavity mode volume approaches 0. However, as L approaches 0 the incident threshold pump power, P_{th}, approaches infinity since no power is absorbed. If instead P_{th} is differentiated with respect to L and minimized, one obtains the condition

$$\frac{f_a N_0 \sigma}{\alpha} = \frac{\exp(-\alpha L)}{1 - \exp(-\alpha L)} (f_a N_0 \sigma L + \delta/2) \quad (8)$$

for minimum incident threshold power. This condition gives a finite L for the minimum in terms of the absorption coefficient at the pump wavelength, the lower laser level population, the round-trip loss, and the stimulated emission cross section. This optimum length is a balance between two conditions: 1) if the laser medium is too short in end-pumping, little pump light is absorbed, and 2) if it is too long, a large portion of the medium remains unpumped with no population inversion. This optimum length is also important because it helps to minimize the parasitic oscillation problem in Nd^{3+} lasers.

Fig. 2 shows the optimum length and incident threshold power for the 946 nm transition at room temperature in Nd:YAG as a function of α and δ. It was assumed that τ is 230 μs, f_a is 0.0074, f_b is 0.6, η_p is 1, the cavity mode and pump radii are both 20 μm, the pump wavelength is 808 nm, and N_0 is 1.5×10^{20} cm^{-3}. The stimulated emission cross section as well as the absorption cross section were taken to be 4×10^{-20} cm^2 although there is evidence that the former is up to 25 percent larger than the latter in Nd:YAG [24]. The absorption coefficient at the pump was varied from 2 to 8 cm^{-1} and the loss from 0.1 to 2.4 percent. The incident threshold power if the length of the crystal is taken to be $1/\alpha$ is plotted in the dashed lines for comparison in Fig. 2(b).

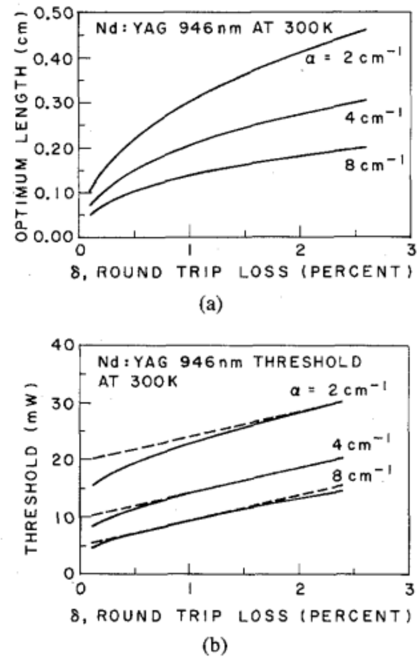

Fig. 2. (a) Optimum length and (b) calculated thresholds for a 946 nm at 300 K Nd:YAG laser as a function of the round-trip losses and absorption coefficient at the pump wavelength. Solid lines in (b) are for the optimum length and dashed lines are for a crystal length of $1/\alpha$.

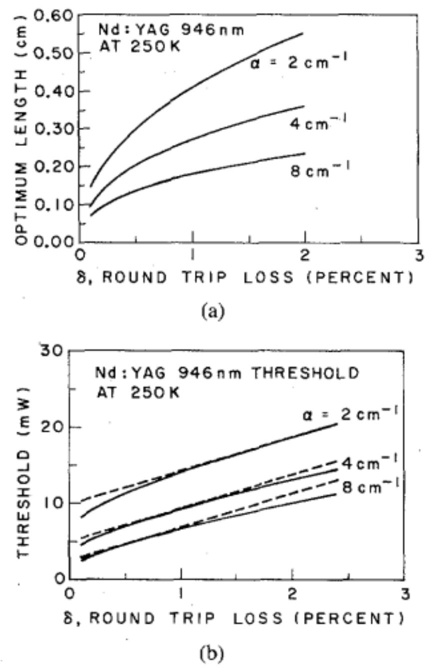

Fig. 3. Same as Fig. 2 except for ~250 K.

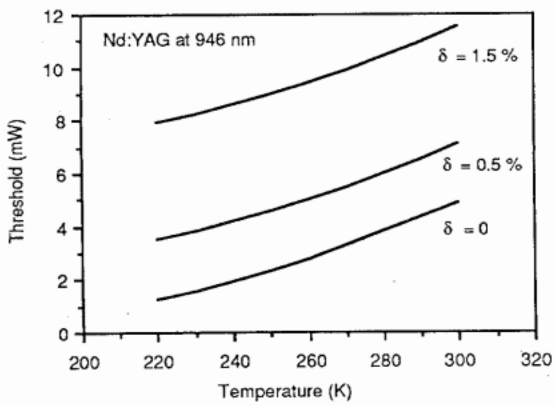

Fig. 4. Threshold as a function of temperature and round-trip cavity loss for 946 nm Nd : YAG transition.

Fig. 3 shows the same calculation if f_a is taken to be 0.0037 which corresponds to a temperature of about 250 K. While σ and f_b also change with temperature, they are taken to be the same at this reduced temperature since their changes are small compared to that for f_a. These plots indicate that for low threshold, it is important to have high absorption at the pump. They also indicate that a laser medium length one inverse absorption long at the pump wavelength gives a reasonable approximation to the optimum length for Nd:YAG 946 nm transition. Fig. 4 shows the calculated incident threshold power as a function of temperature for a fixed value of $\alpha = 8\ \text{cm}^{-1}$ and various values of cavity loss. The length of the gain medium is taken to be $1/\alpha$, and the cavity mode and pump are taken to have Gaussian beam radii of 20 μm. From the plots in Figs. 2–4 it is clear that thresholds are low enough that diode pumping this transition is a realistic possibility. All the calculations for threshold assume that the pump radiation is only single-passed through the gain medium, but it may be possible in some cases to double pass the pump by retroreflection. Significant lowering of threshold can be expected in this case. For example, if the pump is double-passed and the gain medium is made half as long as for the single-pass case, the contribution to the threshold due to the lower laser level population is halved.

C. Output Modeling

We next model the quasi-three-level output above threshold. For this calculation, a mode overlap approach is taken [18]. Under the assumptions that the populations of the energy levels within each manifold can be taken to be in quasi-thermal equilibrium at all times, in steady state the rate equations for the populations of the upper and lower laser levels and the cavity photon number are

$$\frac{dN_b(r, z)}{dt} = f_b R r_p(r, z) - \frac{N_b(r, z) - N_b^o}{\tau} - \frac{f_b c\sigma[N_b(r, z) - N_a(r, z)]}{n} S s_0(r, z) = 0 \quad (9a)$$

$$\frac{dN_a(r, z)}{dt} = -f_a R r_p(r, z) - \frac{N_a(r, z) - N_a^o}{\tau} + \frac{f_a c\sigma[N_b(r, z) - N_a(r, z)]}{n} S s_0(r, z) = 0 \quad (9b)$$

where

c = speed of light
S = cavity photon number
n = index of refraction
N_a^o, N_b^o = populations of levels a and b at thermal equilibrium.

The first two of these equations can be combined into one equation in terms of the population inversion

$$\frac{d\Delta N(r, z)}{dt} = (f_b + f_a) R r_p(r, z) - \frac{\Delta N(r, z) - \Delta N^o}{\tau} - \frac{(f_b + f_a) c\sigma \Delta N(r, z)}{n} S s_0(r, z) = 0 \quad (10)$$

where $\Delta N = N_b - N_a$, and ΔN^o is the equilibrium population inversion. This equation differs from the traditional three-level laser calculation in that the pump rate is not considered to be proportional to the lower state population. This is a consequence of assuming no saturation of the ground state manifold. Another equation describes the cavity photon number, S, and is given by

$$\frac{dS}{dt} = 0 = \frac{c\sigma}{n} \iiint \Delta N(r, z)\, S s_0(r, z)\, dV - \frac{c\delta}{2nL} S \quad (11)$$

where δ is the cavity loss including output coupling. Solving (10) for ΔN and substituting into (11), one obtains

$$\frac{\delta}{2\sigma L} = (f_b + f_a) R\tau \iiint \frac{r_p(r, z)\, s_0(r, z)}{1 + \frac{(f_b + f_a) c\sigma\tau}{n} S s_0(r, z)} dV + \Delta N^o \iiint \frac{s_0(r, z)\, dV}{1 + \frac{(f_b + f_a) c\sigma\tau}{n} S s_0(r, z)} \quad (12)$$

which gives a relation between the pump rate R and the cavity photon number S. Equation (12) is identical to the four-level laser equation except that the second integral containing ΔN^o is an additional term. This can be seen by setting $\Delta N^o = 0$ which is the four level laser case. We consider only the case $w_p \leq w_0$ since for $w_p > w_0$ the slope efficiency and therefore overall efficiency decreases rapidly [20]. For this case, the first integral in (12) can be solved analytically if $(w_0/w_p)^2$ is an integer. The second integral can also be solved analytically. It is convenient to define

$$\frac{1}{S'} = \frac{(f_b + f_a)c\sigma\tau}{n\pi w_0^2 L} \tag{13}$$

where S' is equivalent to a saturation photon number. Solving the integrals in (12) and using (13) yields

$$\frac{\delta}{2\sigma L} - \frac{\Delta N^o S'}{2S} \ln\left(1 + \frac{2S}{S'}\right) = \frac{-2(f_b + f_a)R\tau p}{\pi w_0^2 L}\left[\sum_{k=1}^{p} \frac{(-1)^k}{(p-k+1)(2S/S')^k} + \frac{(-1)^{p+1}}{(2S/S')^{p+1}} \ln\left(1 + \frac{2S}{S'}\right)\right] \tag{14}$$

where $p = (w_0/w_p)^2$. The term with ΔN^o in (12) has been brought to the left-hand side. The only difference between this solution and the four-level laser solution is this term. Rewriting the LHS of the equation in the form

$$\frac{\delta}{2\sigma L} - \frac{\Delta N^o S'}{2S} \ln\left(1 + \frac{2S}{S'}\right) = \frac{1}{2\sigma L}\left[\delta - \frac{\Delta N^o L\sigma S'}{S} \ln\left(1 + \frac{2S}{S'}\right)\right] \tag{15}$$

we can see that the extra term due to the lower laser level population can be interpreted as a saturable loss. This saturable loss term can be written in terms of the saturation intensity, I_{sat}, for the transition which is

$$I_{\text{sat}} = \frac{h\nu}{(f_b + f_a)\sigma\tau} \tag{16}$$

and the circulating intensity, I, averaged over the Gaussian beam

$$I = \frac{Sch\nu}{\pi w_0^2 nL} \tag{17}$$

where $h\nu$ is the photon energy of the laser. Taking into account that the power flows both directions in the cavity, the saturable loss term, δ_s, becomes

$$\delta_s = -\frac{\Delta N^o L\sigma S'}{S} \ln\left(1 + \frac{2S}{S'}\right) = -\frac{\sigma\Delta N^o L I_{\text{sat}}}{I} \ln\left(1 + \frac{2I}{I_{\text{sat}}}\right). \tag{18}$$

This additional variable loss term causes a decrease in slope efficiency, η, which is proportional to the ratio $T/(\delta + \delta_s)$ where T is the output coupling, compared to that in a four-level laser in which δ_s is 0.

There are two important limits for δ_s. For low-circulating intensity, $2I/I_{\text{sat}} \ll 1$, this loss can be approximated as

$$\delta_s \approx -2\delta\Delta N^o L. \tag{19}$$

So the saturable loss is equal to the residual absorption due to the lower laser level population at low-circulating intensities. The second important limit is the case where this saturable loss is negligible or

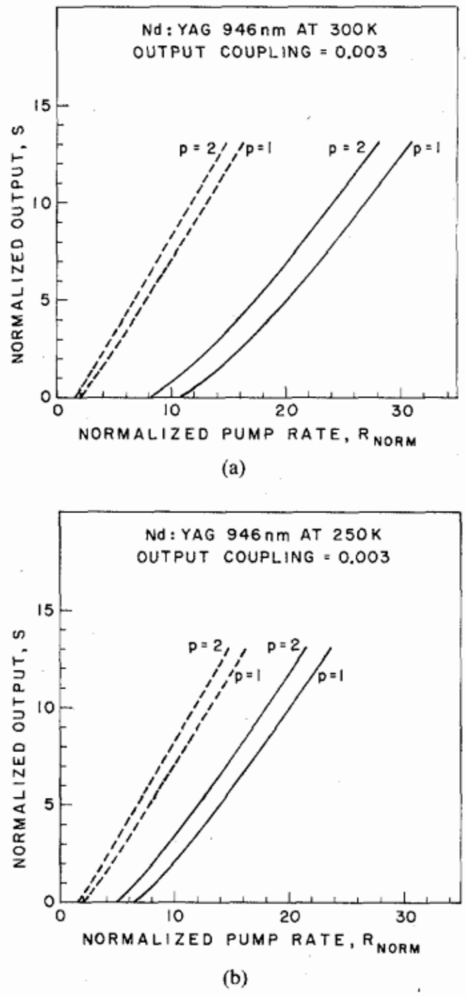

Fig. 5. Normalized output for zero and finite lower laser level populations. Dashed lines are for no lower level population. Parameters assumed are that for the 946 nm transition in Nd:YAG. (a) 300 K. (b) 250 K.

$$\delta \gg \delta_s \tag{20}$$

and the slope efficiency is essentially the same as for a four-level laser.

The output of this laser can be calculated and compared to that for the four level laser case. The number of output photons per unit time, S_o, in terms of the cavity photon number is

$$S_o = \frac{TSc}{2nL}. \tag{21}$$

It is convenient to define a normalized pumping parameter, R_{norm}, which is given by

$$R_{\text{norm}} = \frac{\pi w_0^2 \delta}{4\sigma f_b \eta_p \tau}. \tag{22}$$

This is the pump rate for threshold if the pump spot size is infinitesimally small. Then, a normalized pump rate, $F = R/R_{\text{norm}}$, and a normalized output, $s = S_o/R_{\text{norm}}$, can be defined [21], [23].

TABLE I
QUASI-THREE-LEVEL LASER TRANSITION IN YAG

Ion	Transition	Wavelength (μm)	Terminal level (cm^{-1})	f_a @ 300 K	Ref.
Nd^{3+}	$^4F_{3/2}$–$^4I_{9/2}$	0.946	857	0.0074	[25]
Ho^{3+}	$^5I_7$–$^5I_8$	2.129	532	0.012	[26], [27]
Er^{3+}	$^4I_{13/2}$–$^4I_{15/2}$	1.632	426	0.036	[28], [29]
Tm^{3+}	$^3F_4$–$^3H_6$	2.019	~600	0.012	[30], [31]

Fig. 5(a) shows a comparison the output for a laser with some lower laser level population to that with $\Delta N^o = 0$ using the parameters for the 946 nm transition of Nd:YAG at room temperature. Fig. 5(b) is the same except at 250 K. The output coupling is 0.3 percent and is taken to be the only cavity loss, the spot size in the cavity is taken to be 20 μm, and the length of the gain medium is taken to be 0.15 cm. Clearly, the slope efficiency is reduced by the residual lower laser level population. However, as seen in Fig. 5(b), device performance can be improved by cooling.

These results are valid for quasi-three-level laser systems where N_1, the population in the upper laser level manifold, is small compared to the total doping level N_0. This is generally true for transitions to ground-state manifolds in which the lower laser level has a relatively small thermal occupation. Table I lists some laser transitions of ions in YAG where this model would be applicable. Some of the numbers for f_a are estimates because the entire energy level diagram for the ground-state manifold is not entirely known.

III. Experimental Results

We have demonstrated CW laser oscillation on the 946 nm Nd:YAG transition by end-pumping. As previously mentioned, there have been a number of difficulties in operating this laser because of the relatively low gain of this transition compared to that at 1.06 μm and the residual lower laser level population at room temperature. These difficulties can be overcome with appropriate design of the laser. A rhodamine 6G dye laser at 588 nm was chosen as the pump source to emulate a diode laser. Threshold is highly dependent on the absorption coefficient at the pump wavelength as indicated by the previous calculations, but the absorption coefficients at 588 and 808 nm are nearly equal.

A schematic diagram of the experimental apparatus is shown in Fig. 6. The crystal used in the experiment was polished with a 1.8 cm radius of curvature on one face and a flat on the other. The curved face was coated with a high reflector mirror and the flat with a single-layer antireflection coating both at 946 nm. The rod was 1.5 mm long, and the Nd-doping was 1.1 at mole percent. The doping level is not critical in the end-pumping geometry since both the absorption coefficient and lower state population scale proportionately with doping, so the rod length can also be scaled accordingly. However, higher doping does allow the design of shorter resonators with smaller mode volumes. The absorption coefficient was measured to be ~ 8.5 cm^{-1} at the pump wavelength. The cavity was formed by this rod and an output coupler with a 10 cm radius of curvature and nominally 0.3 percent transmittance. The space between the rod and output coupler was nominally 10 cm, which made the Gaussian beam radius in the rod to be ~ 20 μm. The pump beam was focused into the rod with a 3.5 cm focal length lens, which led to ~ 20 μm radius spot in the rod. For these measurements, the pump beam was chopped to reduce heating effects although true CW operation was obtained. Typically, the duty cycle was 10–25 percent, and the on time was 5 ms.

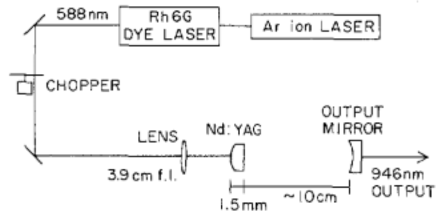

Fig. 6. Diagram of the experimental apparatus.

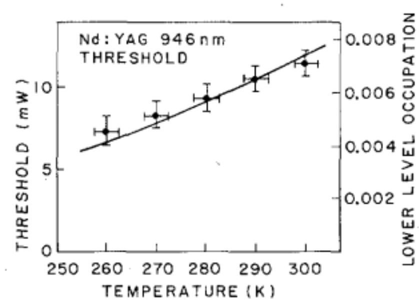

Fig. 7. Incident threshold pump power and lower laser level fractional occupation as a function of temperature for Nd:YAG 946 nm transition. The individual data points are the threshold measurements and the line is the occupation.

Fig. 7 shows a plot of the incident threshold pump power as well as the fractional occupation of the lower laser level as a function of temperature. The threshold at room temperature is slightly higher than the 8.6 mW predicted by (7) if the loss is assumed to be due to the output coupling only. This is probably due to a small amount of other cavity losses. The close fit of the temperature dependence of threshold with lower laser level occupation indicates that the population in the lower laser level as opposed to the other cavity losses is the dominant term in determining threshold given in (7). This is in agreement with the model because in (7), the term $\sigma f_a N_0 L$ is 0.0067 and $\delta/2$ is near 0.0015 if the output coupling is the largest other loss. These threshold numbers should be indicative of what should be possible under diode laser pumping, so the demonstrated threshold is certainly low enough that diode laser pumping of this transition is possible [32].

Fig. 8 shows output power at 946 nm as a function of absorbed pump power at room temperature for this laser. Up to 4 mW of output for 82 mW of absorbed power was

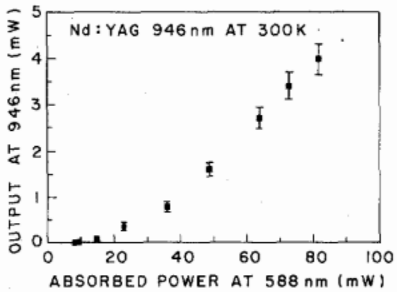

Fig. 8. Output power at 946 nm as a function of absorbed pump power at 588 nm.

demonstrated and a least squares fit to the highest five data points gives a slope efficiency of 7 percent. The slope efficiency appear to be limited by the low value of output coupling. Since the contribution to threshold is dominated by the lower laser level term and cavity losses other than output coupling, the output coupling could be raised to increase slope efficiency with only a small increase in threshold. The laser operated in a TEM_{00} transverse mode.

Diffraction loss in this cavity also limited slope efficiency. In order to have a small spot size in the rod, the spacing between the output mirror and laser rod was such that the resonator was at the edge of cavity stability. The small spot size reduces threshold and decreases the variable loss, δ_s, by raising the circulating intensity. However, as the spot size decreased at the rod it increased at the output coupler. At the lowest threshold for 946 nm, this spot is large enough for some diffraction loss to occur around the half inch diameter of the output coupler. It was possible to have the cavity spacing such that even smaller spot sizes in the rod could be attained in this cavity, but the threshold increased and slope efficiency decreased due to increased diffraction loss. As the cavity length was adjusted allow even smaller spot sizes in the rod, parasitic oscillation at 1.06 μm was observed. Diffraction loss affects 946 nm operation more than 1.06 μm operation because the gain to loss ratio at 946 nm is reduced more than at 1.06 μm due to the lower stimulated emission cross section. Since it is the gain to loss ratio that determines threshold, when the diffraction loss becomes large enough, this ratio becomes more favorable for 1.06 μm than for 946 nm, and the laser begins to operate at 1.06 μm. The diffraction loss can be avoided with a larger output mirror, for example, so lower thresholds and higher slope efficiencies than those demonstrated here could be expected.

This parasitic oscillation at 1.06 μm is not a fundamental difficulty under CW oscillation and can be avoided with proper design. Round-trip losses in this cavity at 1.06 μm due to mirror transmission are estimated to be 60 percent and with appropriate coating design this loss can be increased. The needed round-trip loss to hold-off 1.06 μm oscillation can be found from (7) using the condition P_{th} (946 nm) $< P_{th}$ (1.06 μm). However, it is important to note that (7) is only valid in the low-gain approximation, so as the round-trip losses increase this approximation becomes worse. Given the spectroscopic parameters for each transition and the loss at 946 nm, one can calculate the required loss at 1.06 μm to avoid 1.06 μm oscillation. The effective stimulated emission cross section at 946 nm in Nd:YAG is estimated to be 1/10th that at 1.06 μm [24]. Consequently, the losses at 1.06 μm must be at least 10 times that at 946 nm. This ratio does not account for the lower laser level population, so this required loss ratio between that at 1.06 μm and 946 nm increases as the rod length increases. This shows the importance of high pump absorption and optimum length in holding-off 1.06 μm oscillation.

IV. Summary

We have demonstrated laser operation on the $^4F_{3/2}$–$^4I_{9/2}$ transition in Nd:YAG with low threshold, and we have modeled the threshold and operation above threshold for this laser. In modeling this laser as well as other lasers with lower laser level population at equilibrium, the lower laser level population can be treated as saturable loss which decreases as the circulating intensity increases. Further improvement in laser operation should be possible by designing the cavity mode volume to be smaller which decreases threshold and increases the circulating intensity. In the future, diode pumping of this transition could be tried as well as intracavity doubling to the blue. Such a source could be a replacement for low-power argon-ion lasers. Other Nd-doped materials may work better than YAG on this transition. For example, Nd:$Lu_3Al_5O_{12}$ has a larger ground state splitting and therefore a smaller fractional occupation of the lower laser level. However, we do not know the other important spectroscopic parameters such as the absorption coefficient at the pump and the stimulated emission cross section. Modeling of this quasi-three-level laser applies to others such as the $^3F_4$–$^3H_6$ transition in Tm^{3+} or the $^5I_7$–$^5I_8$ transition in Ho^{3+}. These lasers are often operated at liquid nitrogen temperatures as four level lasers; this model provides us a tool in understanding room temperature operation of these lasers.

References

[1] L. F. Johnson and R. A. Thomas, "Maser oscillations at 0.9 and 1.35 microns in $CaWO_4$:Nd^{3+}," *Phys. Rev.*, vol. 131, pp. 2038–2040, 1963.

[2] R. W. Wallace and S. E. Harris, "Oscillation and doubling of the 0.946 μ line in Nd^{3+}:YAG," *Appl. Phys. Lett.*, vol. 15, pp. 111–112, 1969.

[3] M. Birnbaum, A. W. Tucker, and P. J. Pomphrey, "New Nd:YAG laser transitions $^4F_{3/2} \rightarrow {}^4I_{9/2}$," *IEEE J. Quantum Electron.*, vol. QE-8, p. 501, 1972.

[4] M. Birnbaum, A. W. Tucker, and C. L. Fincher, "cw room temperature laser operation of Nd:CAMGAR at 0.941 and 1.059 μ," *J. Appl. Phys.*, vol. 49, pp. 2984–2985, 1978.

[5] I. Alcock, A. I. Ferguson, D. C. Hanna, and A. C. Tropper, "Continuous-wave oscillation of a monomode neodymium-doped fibre laser at 0.9 μm on the $^4F_{3/2} \rightarrow {}^4I_{9/2}$ transition," *Opt. Commun.*, vol. 58, pp. 405–408, 1986.

[6] H. Po, F. Hakimi, R. J. Mansfield, R. P. Tumminelli, B. C. McCollum, and E. Snitzer, "Neodymium fiber lasers at 0.905, 1.06, and 1.4 μm," in *Tech. Dig., Opt. Soc. Amer. Ann. Meet.*, Optical Society of America, Washington, DC, 1986, p. 121.

[7] B. Zhou, T. J. Kane, G. J. Dixon, and R. L. Byer, "Efficient, frequency-stable laser-diode pumped Nd : YAG laser," *Opt. Lett.*, vol. 10, pp. 62–64, 1985.

[8] D. L. Sipes, "Highly efficient neodymium: Yttrium aluminum garnet laser end pumped by a semiconductor laser array," *Appl. Phys. Lett.*, vol. 47, pp. 74–76, 1985.

[9] S. R. Chinn, "Intracavity second-harmonic generation in a Nd pentaphosphate laser," *Appl. Phys. Lett.*, vol. 29, pp. 176–178, 1976.

[10] T. Baer and M. S. Keirstead, "Intracavity frequency doubling of a Nd : YAG laser pumped by a laser diode array," in *Dig. Conf. Lasers, Electro-Opt.*, Opt. Soc. Amer., Washington, DC, 1985, paper ThZZ1.

[11] T. Y. Fan, G. J. Dixon, and R. L. Byer, "Efficient GaAlAs diode-laser-pumped operation of Nd : YLF at 1.047 μm with intracavity doubling to 523.6 nm," *Opt. Lett.*, vol. 11, pp. 204–206, 1986.

[12] —, "Diode-pumped intracavity doubled Nd : YLF laser," in *Dig. Conf. Lasers, Electro-opt.*, Opt. Soc. Amer., Washington, DC, 1986, paper TuK22.

[13] F. W. Ostermayer, "LED end-pumped Nd : YAG lasers," *IEEE J. Quantum Electron.*, vol. QE-13, pp. 1–6, 1977.

[14] K. Otsuka and T. Yamada, "Resonant absorption in $LiNdP_4O_{12}$ lasers," *Opt. Commun.*, vol. 17, pp. 24–27, 1976.

[15] S. R. Chinn, "Thermal behavior of NdP_5O_{14} lasers," *J. Appl. Phys.*, vol. 53, pp. 5471–5478, 1982.

[16] H. Statz and C. L. Tang, "Multimode oscillations in solid-state masers," *J. Appl. Phys.*, vol. 35, pp. 1377–1383, 1964.

[17] H. G. Danielmeyer, "Stoichometric laser materials," *Festkorperprobleme XV*, pp. 253–277, 1975.

[18] K. Kubodera and K. Otsuka, "Single-transverse-mode $LiNdP_4O_{12}$ slab waveguide laser," *J. Appl. Phys.*, vol. 50, pp. 653–659, 1979.

[19] K. Kubodera, K. Otsuka, and S. Miyazawa, "Stable $LiNdP_4O_{12}$ miniature laser," *Appl. Opt.*, vol. 18, pp. 884–890, 1979.

[20] G. Huber, "Miniature neodymium lasers," in *Current Topics in Materials Science, Vol. 4.* Amsterdam, The Netherlands: North Holland, 1980, pp. 1–45.

[21] D. G. Hall, R. J. Smith, and R. R. Rice, "Pump-size effects in Nd : YAG lasers," *Appl. Opt.*, vol. 19, pp. 3041–3043, 1980.

[22] M. J. F. Digonnet and C. J. Gaeta, "Theoretical analysis of optical fiber laser amplifiers and oscillators," *Appl. Opt.*, vol. 24, pp. 333–342, 1985.

[23] P. F. Moulton, "An investigation of the Co : MgF_2 laser system," *IEEE J. Quantum Electron.*, vol. QE-21, pp. 1582–1595, Oct. 1985.

[24] B. F. Aull and H. P. Jenssen, "Vibronic interactions in Nd : YAG resulting in nonreciprocity of absorption and stimulated emission cross sections," *IEEE J. Quantum Electron.*, vol. QE-18, pp. 925–930, May 1982.

[25] G. A. Bogamolova, L. A. Bumagina, A. A. Kaminskii, B. Z. Malkin, "Crystal field in laser garnets with TR^{3+} ions in the exchange charge model," *Sov. Phys. Solid State*, vol. 19, pp. 1428–1435, 1977.

[26] L. F. Johnson, J. E. Geusic, and L. G. Van Uitert, "Efficient, high-power, coherent emission from Ho^{3+} ions in yttrium aluminum garnet assisted by energy transfer," *Appl. Phys. Lett.*, vol. 8, pp. 200–202, 1966.

[27] M. K. Ashurov, Yu. K. Voron'ko, E. V. Zharikov, A. A. Kaminskii, V. V. Osiko, A. A. Sobol', N. I. Timoshechkin, V. A. Fedorov, and A. A. Shabaltai, "Structure, spectroscopy, and stimulated emission of crystals of yttrium holmium aluminum garnets," *Inorgan. Mat.*, vol. 15, pp. 979–983, 1979.

[28] G. M. Zverev, V. M. Garmash, A. M. Onishchenko, V. A. Pashkov, A. A. Semonov, Yu. M. Kolbatskov, and A. I. Smirnov, "Induced emission by trivalent erbium ions in crystals of yttrium-aluminum garnet," *J. Appl. Spec.*, vol. 21, pp. 1467–1469, 1974.

[29] N. I. Agladze, A. A. Balashov, G. N. Zhizhin, and M. N. Popova, "High resolution spectra in the $^4I_{15/2} \rightarrow {}^4I_{13/2,11/2}$ transition region for an erbium-activated-YAG crystal," *Opt. Spectros.*, vol. 57, pp. 228–229, 1984.

[30] L. F. Johnson, J. E. Geusic, and L. G. Van Uitert, "Coherent oscillations from Tm^{3+}, Ho^{3+}, Yb^{3+}, and Er^{3+} ions in yttrium aluminum garnet," *Appl. Phys. Lett.*, vol. 7, pp. 127–129, 1965.

[31] G. M. Zverev, G. Ya. Kolodnyi, and A. M. Onishchenko, "Resonant and nonresonant processes of excitation energy transfer from Tu^{3+} or Ho^{3+} ions to the Er^{3+} ions in $(Y,Er)_3Al_5O_{12}$ crystals," *Sov. Phys.-JETP*, vol. 57, pp. 435–440, 1970.

[32] Since this paper was submitted, we have demonstrated diode laser pumping on this transition.

Tso Yee Fan (S'83) was born in Manhattan, KS, in 1959. He received S.B. degrees from the Massachusetts Institute of Technology, Cambridge, MA, in both electrical engineering and materials science and engineering in 1981 and the M.S. degree from Stanford University, Stanford, CA, in 1983.

Since 1983 he has been working towards the Ph.D. degree, also in electrical engineering, at Stanford University, and currently holds an IBM Graduate Fellowship for the 1986–1987 academic year. His research interests include new solid-state laser materials and devices and nonlinear optics.

Mr. Fan is a student member of the Optical Society of America.

Robert L. Byer (M'75–SM'83) received the Ph.D. degree in applied physics from Stanford University, Stanford, CA, in 1969.

After joining the Applied Physics Department at Stanford University, he began research in remote sensing using tunable laser sources. Research in that area led to the development of the unstable resonator Nd : YAG laser and to high-power tunable infrared generation in $LiNbO_3$ parametric tuners. In 1974 he and his colleagues initiated research in coherent anti-Stokes raman spectroscopy (CARS), named the effect, and continued research in high resolution Raman Spectroscopy. In 1976 he suggested the use of stimulated Raman scattering in hydrogen gas to generate 16 μm radiation from a CO_2 laser source. Research at Stanford University confirmed the expected simplicity and efficiency of the approach. In 1980 research on slab geometry solid state laser sources was begun. The program has led to successful theoretical and experimental development in high peak and average power solid-state laser sources. His early and continuing interest has been nonlinear interactions including harmonic generation and parametric oscillators. Research in advanced solid-state laser sources is continuing. He was Chairman of the Applied Physics Department from 1981 to 1984 and was appointed Associate Dean of Humanities and Sciences in 1985. He has worked in industry at Spectra Physics (1964–65), and at Chromatix from 1969 to 1974. He helped found Quanta Ray Inc., in 1975 and Lightwave Electronics Corporation in 1985. He has published more than 140 papers and holds 14 patents in the field of lasers.

Dr. Byer is a member of the American Association for the Advancement of Science and the American Physical Society, is a Fellow of the Optical Society of America, and was President of the IEEE Lasers and Electro-Optics Society for 1985.